Friction **5**(4): 402–413 (2017)
DOI 10.1007/s40544-017-0154-x

ISSN 2223-7690
CN 10-1237/TH

RESEARCH ARTICLE

Tribological behavior of N-doped ZnO thin films by metal organic chemical vapor deposition under lubricated contacts

Bolutife OLOFINJANA[1,3,*], Uchenna Sydney MBAMARA[2], Oyelayo AJAYI[3], Cinta LORENZO-MARTIN[3], Eusebius Ikechukwu OBIAJUUWA[4], Ezekiel Oladele Bolarinwa AJAYI[1]

[1] *Department of Physics and Engineering Physics, Obafemi Awolowo University, Ile-Ife 220005, Nigeria*

[2] *Department of Physics, Federal University of Technology, Owerri, Nigeria*

[3] *Tribology Section, Energy System Division, Argonne National Laboratory, Argonne, IL 60439, USA*

[4] *Center for Energy Research and Development, Obafemi Awolowo University, Ile-Ife 220005, Nigeria*

Received: 30 July 2016 / Revised: 16 October 2016 / Accepted: 14 February 2017

Abstract: N-doped ZnO thin films were deposited on 304L stainless steel through the pyrolysis of zinc acetate and ammonium acetate in different ratios at a temperature of 420 °C using metal organic chemical vapor deposition. Compositional and structural analyzes of the films were performed by using Rutherford backscattering spectroscopy and X-ray diffraction. The frictional behavior of the thin films and 304L stainless steel substrate was evaluated using a ball-on-flat configuration with reciprocating sliding under marginally lubricated and fully flooded conditions. Al alloy (2017) was used as ball counterface, while basestock synthetic polyalfaolefin oil (PAO10) without additives was used as lubricant. The flat and ball counterface surfaces were examined to assess the wear dimension and failure mechanism. Under marginally lubricated condition, N-doped ZnO thin films provided significant reduction in friction, whereas the films have minimal or no effect in friction under fully flooded condition. N-doped ZnO thin films showed a significant effect in protecting the ball counterface as wear volume was reduced compared with that of the substrate under the marginally lubricated condition. Under the fully flooded condition, with the exception of one of the films, the wear volume of the N-doped ZnO thin films ball reduced compared with that of the substrate. In all the ball counterfaces for N-doped ZnO thin films under both conditions, wear occurred through abrasive mechanism of various degrees or mild polishing. Thus, superfluous lubrication of N-doped ZnO thin films is not necessary to reduce friction and wear.

Keywords: ZnO film; metal organic chemical vapor deposition; friction; wear; optical microscopy

1 Introduction

The most common friction and wear reduction approach is lubrication, which involves the application of lubricants between moving surfaces to partially or fully separate contacting surface asperities. Adequate lubrication can be achieved by the use of liquid (oils and greases), solid (thin film coatings), or gas (air bearing). Most oil lubricants used for friction and wear reduction are usually formulated with additives to improve performance [1]. Such oils normally consist of a basestock (which can be synthetic or mineral based) and additive packages. Nanoparticles and submicron particles are also good lubricant additives to improve tribological properties [2–6]. Most works on lubricant formulations are devoted to formulating the proper combination of base stock and additives for a particular or desirable function.

Thin film coatings have been considerably utilized as solid lubricants for high-precision systems such as data storage systems, semiconductor devices, MEMS, space application devices, bio-components, machining

* Corresponding author: Bolutife OLOFINJANA, E-mail: olofinb@oauife.edu.ng

tools, and bearing gears. To achieve adequate lubrication, solid lubricants in the form of thin films need to possess low shear strength to effectively carry the pressure generated between opposing surfaces, thereby reducing friction and wear. Examples of thin films used as solid lubricants are diamond-like carbon; h-BN; metal nitrides such as TiN, CrN, TiCN, and AlTiN; layered materials with covalent bonding within layers but weak bonding between layers such as MoS_2, WS_2, and TaS_2; and submicron or nanocrystalline metal oxides.

Generally, lubricious metal oxides are attractive because they typically do not form strong adhesive bonds in tribological contacts and also because they are thermodynamically stable and environmentally friendly. A typical example of these oxides is ZnO. The primary driving force behind the interest in ZnO thin films is their utility in a variety of technological applications. Their electrical, optical, and electrochemical properties, as well as their thermodynamically stable hexagonal wurtzite structure make them useful in UV-light emitting diodes, solar cells, lasers, surface acoustic wave devices, gas sensor, and photocatalytic activities, among others. In addition, several researchers have demonstrated the possible use of ZnO thin film coatings in tribological applications [7–11]. The coefficient of friction of such films is in the range of 0.15 to 0.25 with good wear life over a long cycle. Such enhanced tribological properties were attributed to the nanocrystalline nature of the ZnO films. ZnO nanoparticles have also been used as lubricant additives [12, 13]. Such ZnO nanoparticles showed excellent friction properties because of their submicrometer-scale spherical nature, which changes the contact configuration from sliding to rolling. However, because of the low hardness of such nanoparticles, their antiwear property was poor [12].

The open structure and favorable coordination number of ZnO allow ZnO to be easily doped with external atoms as zinc or oxygen substitutes, thereby permitting the formation of defects that can alter the structure and ultimately lead to improved properties. In some cases, such defects can cause the formation of slip systems that can alter the electronic structure and lower the shear strength, which can improve tribological performance. For instance, alumina-doped ZnO thin film coatings have lower friction and better wear performance than pure ZnO films [14]. The friction and wear mechanism of such doped ZnO thin films was attributed to nanocrystalline features such as the grain population and substoichiometry of the layer. The friction behavior of carbon-ZnO composite coatings was also studied by Penkov et al. [15]. They pointed out that the C–ZnO coatings demonstrated better tribological behavior compared with pure ZnO. Improvement in tribological properties was attributed to better mechanical properties. Compositing ZnO and organic polymers has also been shown to improve tribological performance and thermal stability, as well as nanochemical properties [14–19]. Furthermore, in terms of lubricant additives, compositing ZnO submicrospheres with Al_2O_3 nanoparticles had been shown to notably improve both the friction reduction and antiwear properties [20]. Such improved tribological properties were attributed to the fact that rolling friction became dominant instead of sliding friction, while the micro/nanoparticles squeezed into the grooves on the rubbing surfaces to reduce wear.

Nitrogen is considered the best candidate for doping ZnO [21]. Aside from having the smallest ionization energy among the group V elements, it also has a similar ionic radius as oxygen. Nanosized nitrigen-doped ZnO was prepared through a variety of techniques in the past. Such techniques include sol-gel method [22], microwave synthesis [23], pulsed laser deposition [24, 25], and microemulsion method [26]. Some of these techniques have different deficiencies, ranging from non-uniformity to reproducibility in composition. Techniques such as pulsed laser deposition also require a vacuum system. Over the years, metal organic chemical vapor deposition (MOCVD) has become an important technique for preparing thin films and coatings of various materials essential to advance technology because the technique requires minimum to no post-deposition processing to prepare high-quality films. Another feature of MOCVD is its versatility in coating both simple and complex components with relative ease even at low temperature.

Our group had deposited nitrogen-doped ZnO thin films on 304L stainless steel using MOCVD and explored their tribological behavior under dry contact condition [27]. However, for completeness, an evaluation of nitrogen-doped ZnO thin films under lubricated contact is necessary because some mechanical components use oil lubrication. For effective integration of oil lubricants and nitrigen-doped ZnO thin films, an adequate understanding of interaction between the oil and the thin film is necessary. The interaction could be synergistic, antagonistic, or have no effect at all. Hence, this study seeks to assess the tribological behavior of nitrogen-doped ZnO thin films under lubricated contacts. The films were deposited on 304L stainless steel using MOCVD from combinations of zinc acetate and ammonium acetate precursor. Contacts were lubricated with basestock polyalpha-olefin (PAO10) without additives. The quantity of oil can affect tribological behavior. Thus, tests were conducted under both marginally lubricated and fully flooded conditions.

2 Experimental details

Nitrogen-doped ZnO thin films were prepared by using the pyrolytic method of MOCVD. The schematic diagram of the MOCVD apparatus was used is shown in Fig. 1. The MOCVD setup is a locally adapted design that had been used in previous studies [28–34]. It is simple, cost effective, and suitable for large-scale

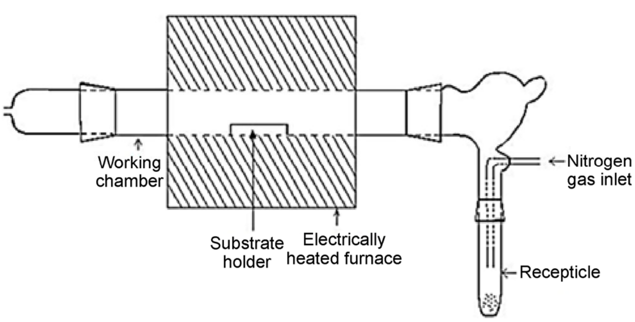

Fig. 1 Schematic diagram of MOCVD apparatus.

production of various thin films for different applications. 304L stainless steel is commonly used for tribological application where corrosion resistance is important and was therefore used as the substrate. A mixture of zinc acetate and ammonium acetate (which serve as the source of nitrogen) was used as the precursor. These two precursors were mixed together in different proportions and grounded thoroughly in a mortar. The fine powder of the precursor was poured into an unheated receptacle, and compressed air was blown through the precursor at a rate of 2.5 dm^3/min. The airborne precursor was transported into the working chamber, which was maintained at 420 °C by an electrically heated furnace. The deposition time was 2 h. Five sets of films, using different ratios of the two precursors, were produced. Table 1 shows the different ratios of the precursor that was used.

The elemental composition, stoichiometry, and thickness of the thin films were determined using Rutherford backscattering spectroscopy (RBS). This procedure was performed by using a 1.7 MeV Tandem accelerator, which involves the use of 1.5 MeV $^4He^+$. The detector scattering angle was 147.7°. The spectrum was obtained under normal condition (angle of incidence $\theta_1 = 0°$ and angle of emergence $\theta_2 = 180°$) with a beam current of 3.8 nA and a nominal beam size of 1 mm. SIMNRA was used to analyze the spectrum that was extracted from the accelerator detector. The X-ray diffraction pattern of the nitrogen-doped ZnO thin films was obtained using MD-10 mini diffractometer with CuK_α radiation. The applied voltage was 25 kV with an exposure time of 1,200 seconds. The intensity data were collected over a diffraction angle, 2θ range of 15° to 50°.

Oil-lubricated friction and wear tests were conducted with a ball-on-flat configuration in reciprocating sliding by using a high-frequency reciprocating rig. The ball

Table 1 Precursor combination, 3-D roughness parameter and thickness of thin films.

Thin Film	Precursor	3-D roughness parameter (nm)	Thickness (nm)
ZO	100% zinc acetate	259.46	185
NZO1	90% zinc acetate + 10% ammonium acetate	162.85	424
NZO2	80% zinc acetate + 20% ammonium acetate	195.66	331
NZO3	70% zinc acetate + 30% ammonium acetate	196.90	253
NZO4	60% zinc acetate + 40% ammonium acetate	157.52	172

counterface was Al alloy (2017) with a diameter of 12.7 mm. The ball's 3D surface roughness parameter (S_a) and hardness are 798 nm and 6.7 GPa ($62R_C$), respectively. The surface statistical properties of nitrogen-doped ZnO thin films were reported earlier [35]. The surface roughness parameters of the films are listed in Table 1. The 304L stainless steel substrate with an isotropic finish similar to that of the thin films (which serves as the baseline) and nitrogen-doped ZnO thin films deposited on 304L stainless steel were tested against the Al alloy (2017) ball. Pure ZnO thin film from 100% zinc acetate, which serves as a control film, was also tested.

The tests were conducted by applying a dead weight of 10 N, which imposes a Hertzian contact pressure of 0.35 GPa. Contacts were lubricated in two ways: marginally lubricated, in which one drop of oil was added at the start of each test, and fully flooded lubrication condition, in which an adequate amount of lubricant was applied to cover the flat surface completely for the entire duration of the test. Basestock synthetic polyalfaolefin oil (PAO10) without additives was used as lubricant. It has a viscosity of 71.1 cSt at 40 °C and a specific gravity of 0.837. The reciprocating frequency was 1 Hz with a stroke length of 20 mm, equivalent to a linear sliding speed of 2 cm/s. All tests were run for 30 minutes in ambient room air (temperature of 25 °C and relative humidity of 65%).

Frictional force was continuously measured during each test from which the coefficient of friction, defined as the ratio of the frictional force to the normal force, was calculated. Wear on flats and ball counterface material was evaluated at the conclusion of each test by using 3D profilometry with an ADE-Phaseshift MicroXam white light optical profilometer. The surface of the flats and the ball counterface were also examined by using an optical microscope to assess the wear and surface damage mechanism.

3 Result and discussion

3.1 Thin films and characterization

Films of good uniformity and adherence were obtained at the deposition temperature of 420 °C. In the hot chamber, the precursor first sublimed before the thermal decomposition, resulting in the coating of the substrate. In the MOCVD process, the deposition involves homogeneous gas phase reactions, which occur in the gas phase, and (or) heterogeneous chemical reaction, which occurs on or near the vicinity of a heated surface, thereby leading to the formation of films.

A typical RBS spectrum of the films is shown in Fig. 2. The spectrum depicts two sections, namely, the substrate section and the coating section, which is around 1,450 keV. The expected elements were detected, with the presence of N, Zn, and O clearly manifested. The stoichiometric ratio of N:Zn:O in all the films was estimated to be 1:5:4, while the thickness ranged between 172 and 424 nm. More detailed analysis of stoichiometry and thickness had been reported earlier [27, 36]. The standard calowear test was also used to measure the thickness of the films. This process involves the creation of a crater by a rotating ball of a known diameter through the film into the substrate. An average value of six different points at different places on the film was taken. The thickness measured by this technique is consistent with that of RBS.

A typical X-ray diffraction pattern of the thin films is shown in Fig. 3. Diffraction peaks occur at various diffraction angles, which correspond to (100), (002), and (101) plane. All the obtained peaks were assigned to the standard hexagonal wurtzite ZnO crystal structure (JCPDS 36-1451). No other peaks that correspond to nitrogen were observed. The presence of these peaks shows that all the films are polycrystalline. The

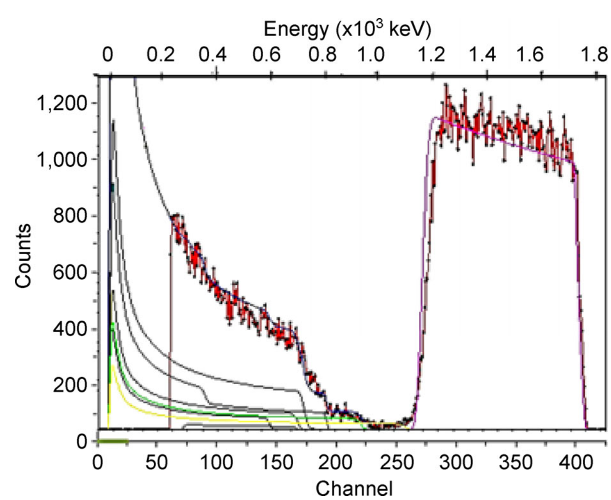

Fig. 2 RBS spectrum of nitrogen-doped ZnO thin film.

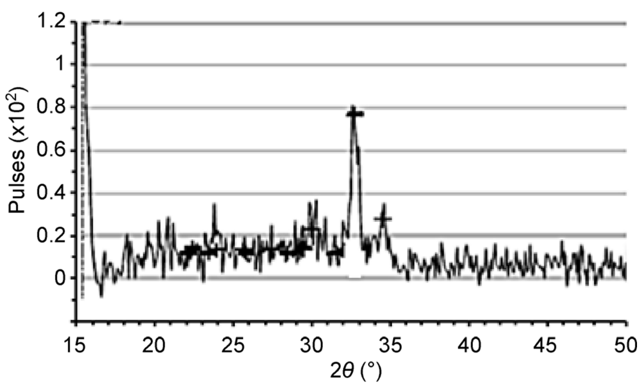

Fig. 3 Typical XRD pattern of nitrogen-doped ZnO thin film.

(002) peak has the highest intensity. The dominance of the (002) peak suggest a highly textured structure in which the *c* axis preferentially aligned perpendicular to the substrate normal. The (002) texture is commonly observed in ZnO films because the *c*-plane perpendicular to the substrate normal is the most densely packed and thermodynamically preferred in the wurtzite structure. The average crystal size of the films based on full width at half maximum (FWHM) of diffraction peaks calculated using Debye–Scherrer equation was 52 and 30 nm for the ZnO thin film and all N-doped ZnO thin films, respectively. The decrease in grain size can be linked to peak broadening, which causes the broadening of FWHM and eventually leads to a decrease in crystallinity. Such peak broadening may be a result of a defect brought about by the incorporation of nitrogen into the ZnO lattice. This result successfully demonstrated that nitrogen can be incorporated into the ZnO thin film lattice by using a combination of zinc acetate and ammonium acetate precursors. The tendency of decreasing grain size and crystallinity with the incorporation of nitrogen in ZnO lattice is similar to that in some previously reported works [26, 37, 38].

3.2 Friction and wear result

The friction behavior of the thin films and the 304L stainless steel substrate (baseline) with reciprocating sliding under both marginally lubricated and fully flooded conditions is shown in Fig. 4. In both the marginally lubricated and fully flooded conditions, a range of friction behaviors were observed. Under the marginally lubricated condition, the substrate showed a friction behavior that is oscillatory in nature, rising and falling at various intervals. The coefficient of friction first increased rapidly at the start of the test to a value of approximately 0.18, followed by a gradual decrease to a value of approximately 0.14 within the first 140 s. Thereafter, the rise and fall continued, which ranged between 0.15 and 0.22. Such frictional behavior can be attributed to the build-up and collapse of the transfer layer [39]. Although this is a lubricated test, the amount of lubricant is marginal, thereby making the operating lubrication regime boundary. Hence, extensive material interaction will still be dominant between the contacting materials through the lubricant film. The contact first produces a high coefficient of friction as a result of the plowing effect, which results in the roughening of the softer material, thereby generating wear debris that can be entrapped. The wear debris accumulates to build up a transfer layer that may become thicker and unstable and eventually collapse. This cycle of buildup and collapse of the transfer layer continued throughout the test, thereby leading to the rise and fall of the coefficient of friction. ZO and NZO1 films showed a similar frictional behavior. The run-in period followed by a fairly stable friction coefficient value that ranges between 0.10 and 0.12 was observed, after which both films showed a transition to unstable higher values (between 0.13 and 0.19) that occurred around 1,300 s. This behavior is mostly likely a result of the wearing-through of films. Similar trends were also observed for the remaining three NZO films (NZO2, NZO3, and NZO4): a run-in period followed by steady-state friction coefficient values between 0.11 and 0.12. Thus, the thin films can evidently provide friction reduction under marginal lubrication. For both ZO and NZO films, such reduction occurred before 1,300 s. The friction reduction in the films can be attributed to the thin films carrying some of the contact load, thus allowing easier sliding between the opposing surfaces. This condition may be a result of the nanocrystalline nature of the films as calculated by the Debye–Scherrer equation [12, 13]. Our result is comparable to that obtained by using sub-microsphere ZnO particles and compositing sub-microsphere ZnO with Al_2O_3 nanoparticles as lubricant additives studied by other authors [12, 13, 20]. Those authors also suggested

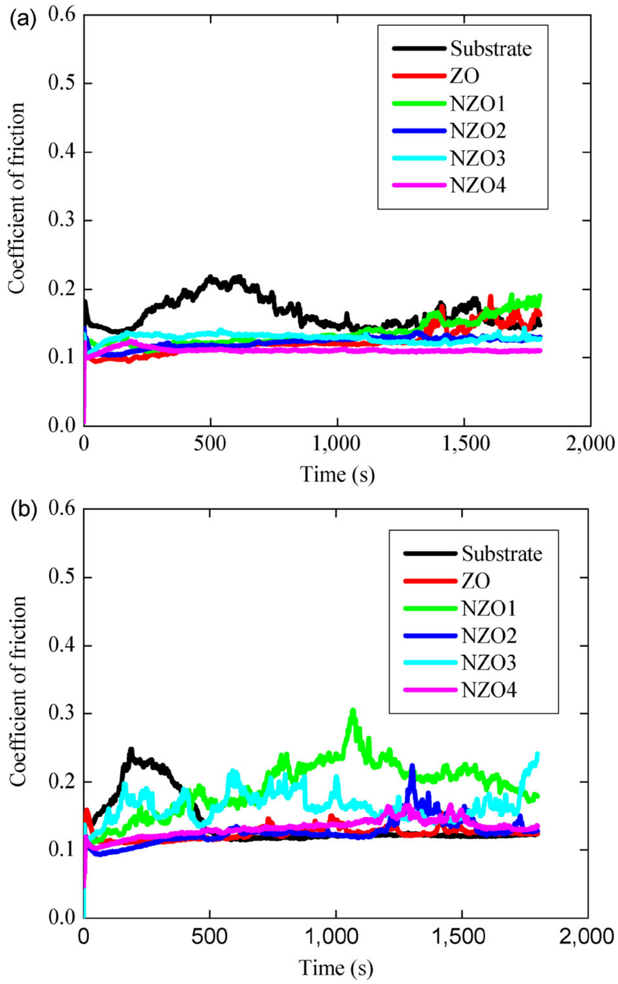

Fig. 4 Coefficient of Friction variation with time under (a) marginally lubricated and (b) fully flooded contact.

that rolling friction became dominant instead of sliding friction, thereby causing the composite micro/nanoparticles to squeeze into the grooves on the rubbing surfaces and reducing friction and wear.

In the fully flooded condition, the coefficient of friction for the substrate increased rapidly to a value of 0.15 at the start of the test, after which it increased gradually to a maximum value of approximately 0.25. After this initial response, the coefficient of friction decreased to a steady-state value of 0.12 in the last 1, 200 s of the test. The initial increase in the coefficient of friction is a result of the run-in process. The steady-state coefficient of friction can be attributed to the extensive formation of a transfer layer on the 304L stainless steel flat, such that after the run-in period, the contacting interface may consist of a sliding aluminum transfer film on the aluminum alloy ball. This type of friction behavior, that is, an initial increase in the coefficient of friction followed by a slow decrease to a constant value, was also observed for aluminum in contact with other materials [40, 41]. During the run-in period, high asperities may be worn down, surface films may be removed, or new films may form [42]. After this period, new changes may occur at the interface of the two sliding surfaces, thereby leading to the formation of a new layer, which may cause a decrease in the coefficient of friction to a new steady-state value. These changes may also include oxidation at the tribocontact interface, thereby resulting in the formation of oxides. Wear debris from the ball may also become trapped at the contact interface. In general, tribolayers consist of a complex mixture of both material pairs in contact, as well as specie from the environment [43]. A steady-state friction coefficient value of 0.11 occurred in ZO within 75 and 650 s. The friction coefficient value then ranged between 0.12 and 0.15 with a stable value of 0.12 in the last 300 s of the test. NZO1 exhibited an unstable friction coefficient ranging between 0.13 and 0.31 throughout the entire duration of the test. For NZO2 film, the steady-state friction coefficient value was approximately 0.11 up to around 1,145 s, after which it showed a noisy pattern followed by a constant value of 0.12 in the last 100 s. NZO3 showed an unstable coefficient of friction, reaching a maximum of 0.24 at the end of the test. The coefficient of friction for NZO4 thin film was similar to that of NZO2. The steady-state value was 0.12 until 1,200 s. The friction showed a slight perturbation between 1,200 and 1,500 s, after which it remained nearly constant at a value of 0.12 within the last 300 s. The perturbation observed in ZO, NZO2, and NZO4 may be a result of some localized damage in the film (as shown in Figs. 8(b) and 13(b)), which can be caused by abrasion. However, after such damage, tribolayer quickly built up on the damage, thereby causing the coefficient of friction to return to a steady state that was observed in the last 100 s and 300 s as the case may be. With this condition, the thin films can provide friction reduction only during the run-in period. Indeed, after the run-in period, during which the tribolayer formed on the substrate, the coefficient of friction for the substrate became lower than that for some of the thin films. Unlike in the marginally lubricated condition, superfluous lubrication of N-doped ZnO thin film is not needed to reduce friction.

At the conclusion of each test, the wear track on both the Al alloy ball counterface and the flat surfaces were characterized by 3D profilometry and optical microscopy. Figures 5–8 show the typical 3D optical profile for flat and ball counterface pairs in marginally lubricated and fully flooded conditions. Most of the wear was produced in the softer counterface (Al alloy ball), and wear on the flats was minimal coupled with evidence of material transfer from the ball counterface. Thus, wear assessment was performed by measuring the wear on the ball counterface for each test. A summary of the wear volume in the balls at the conclusion of the tests for the marginally lubricated (plotted on a log-scale) and fully flooded conditions is shown in Fig. 9. Although no accurate relationship between friction and wear producing realistic result has been defined [44], friction plays an important role in wear volume within a given system. Consequently, the wear behavior of the ball counterface in this study is strongly related to the friction behavior for each flat and ball pair. The wear volume in the ball tested against the thin films is lower than that tested against the substrate under marginally lubricated contact. The thin film-ball pairs also showed lower friction than the substrate-ball pair under the marginally lubricated condition. Under the fully flooded condition, with the exception of NZO1, a reduction in the ball wear volume of the films was observed compared with that of the ball wear volume of the substrate. This result is expected as the friction coefficient of ZNO1 showed unstable behavior, reaching the highest value of 0.31. Thus, the thin films actually protected the ball counterface to a certain extent. The wear reduction could be due to the reduction of shear stress and resultant tensile stresses on the Al alloy ball surface.

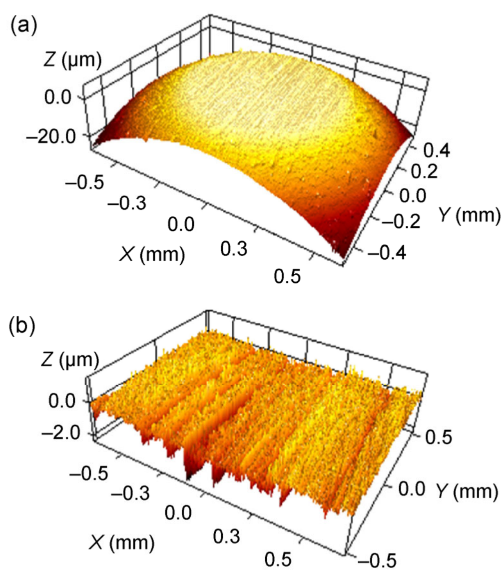

Fig. 5 Typical 3D optical profile of (a) ball counterface and (b) substrate for marginally lubricated condition.

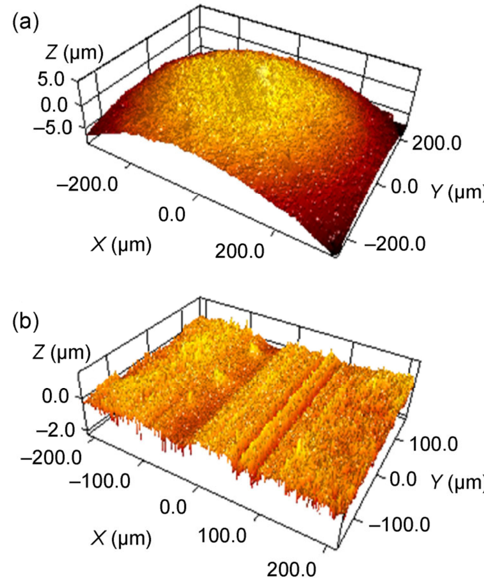

Fig. 6 Typical 3D optical profile of (a) ball counterface and (b) nitrogen-doped ZnO thin film for marginally lubricated condition.

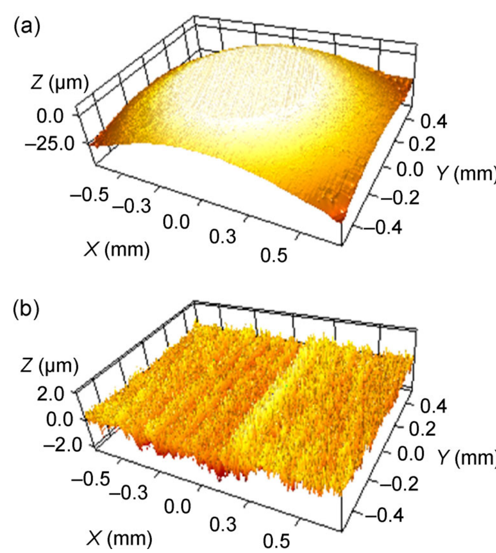

Fig. 7 Typical 3D optical profile of (a) ball counterface and (b) substrate for fully flooded condition.

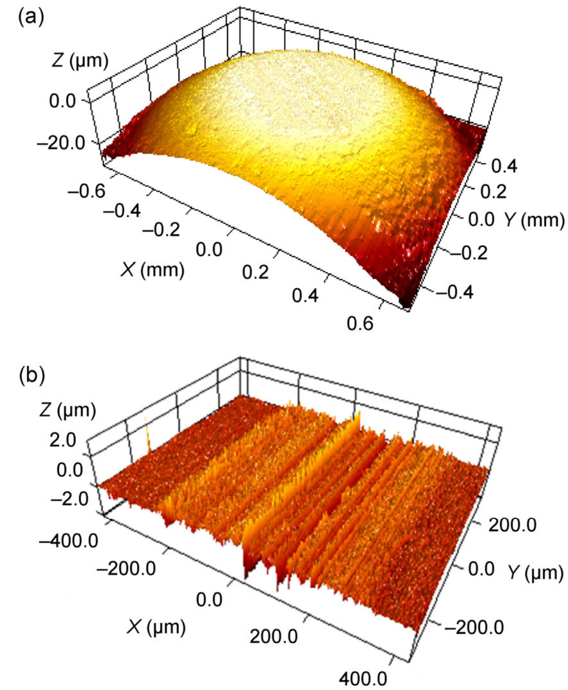

Fig. 8 Typical 3D optical profile of (a) ball counterface and (b) nitrogen-doped ZnO thin film for fully flooded condition.

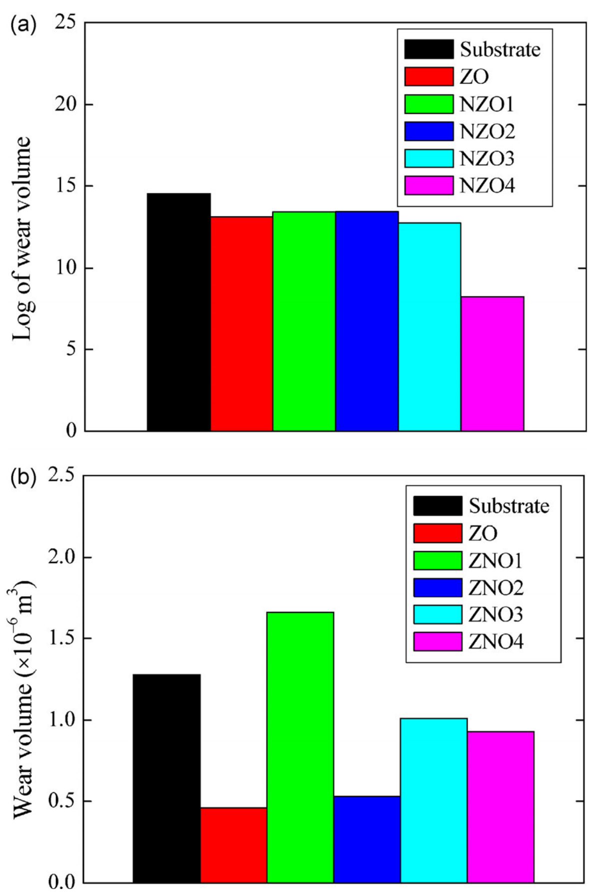

Fig. 9 Ball wear volume after friction test for (a) marginal and (b) flooded condition.

Figures 10–13 show the optical micrographs of wear in the ball and flat pairs under both marginally lubricated and fully flooded conditions. Features observed in the micrographs were similar to those observed in the 3D optical profiles. For substrates tested under both conditions, although wear track is evident, it is for the most part covered by surface films. Such surface films build up and collapse, leading to the rise and fall of the friction coefficient observed in the marginally lubricated test. However, for the fully flooded test, the surface films remain stable, thereby leading to the stable friction coefficient observed in the last 1,200 s of the test. For the thin films tested under both under marginally and fully flooded conditions, evidence of material transfer from the ball exists.

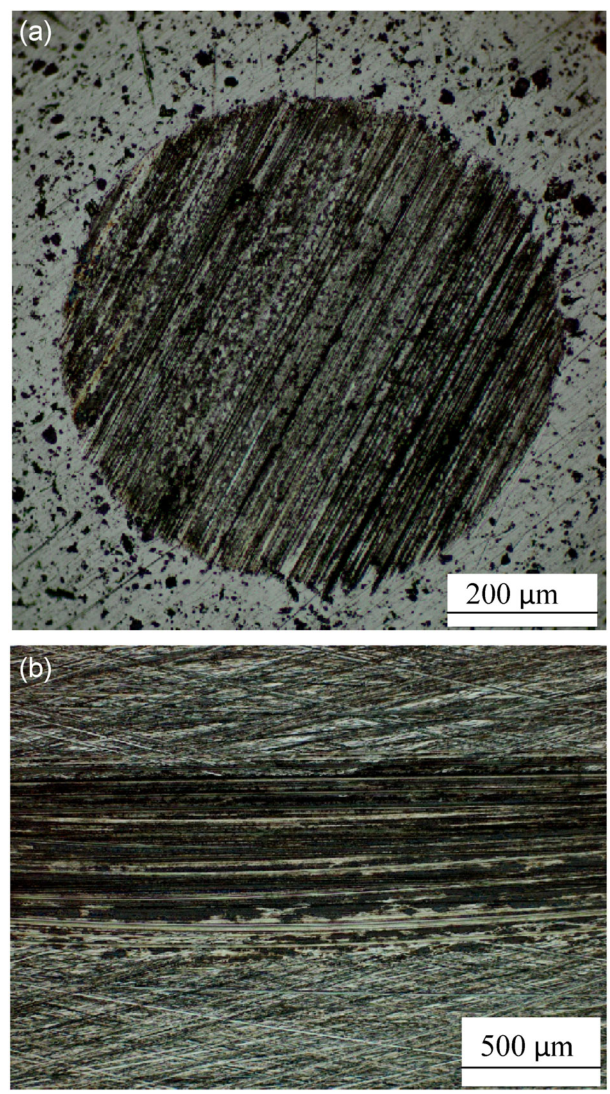

Fig. 10 Optical micrograph of (a) ball counterface and (b) substrate under marginally lubricated condition.

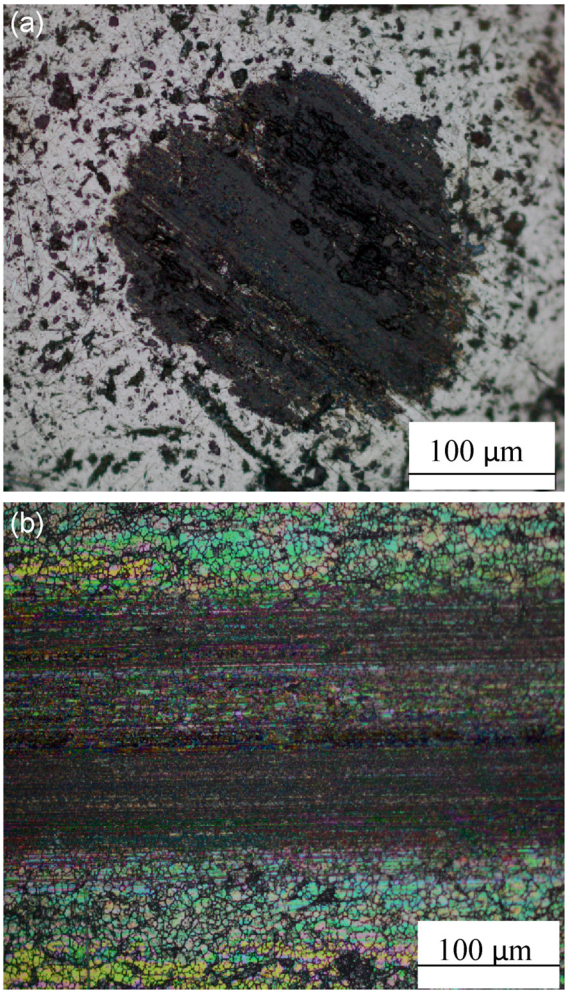

Fig. 11 Typical optical micrograph of (a) ball counterface and (b) nitrogen-doped ZnO thin film under marginally lubricated condition.

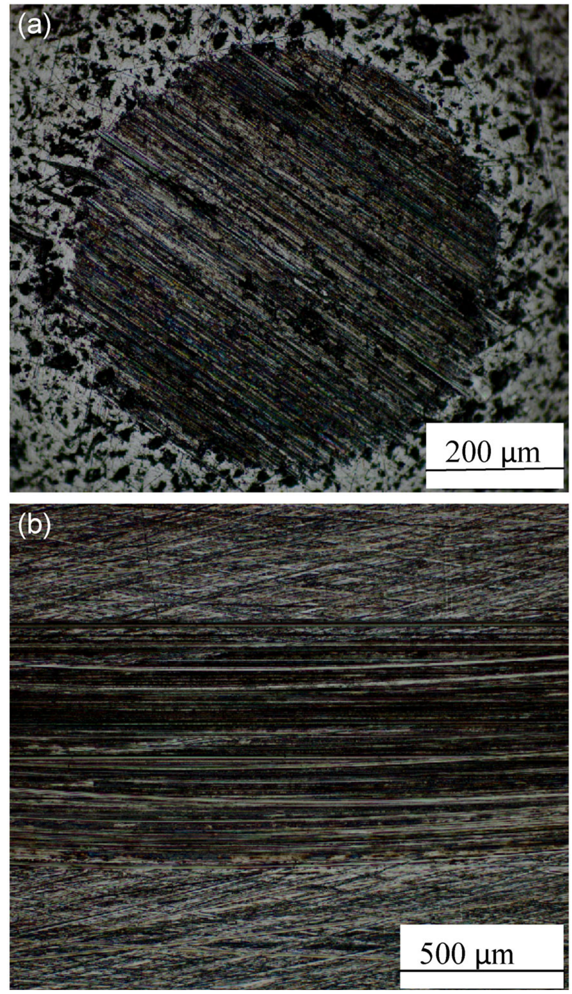

Fig. 12 Optical micrograph of (a) ball counterface and (b) substrate under fully flooded condition.

Some localized damage, which can occur either by abrasion (as indicated by scratches in the direction of sliding) or mild polishing, can also be seen. Different mechanisms and kinetics of material transfer from the ball counterface that occurred during sliding could lead to material build-up on the flats. For instance, after the films had been worn through, the ball comes in contact with the substrate, thereby causing substantial damage and material removal from the ball, which can then be re-deposited on the substrate. The removal of the film coincided with the increase in the coefficient of friction observed in some of the friction behavior because the ball is now sliding against the 304L stainless at this point. A transfer layer may then build up, which accounts for the steady-state coefficient of friction observed in the last 100 or 300 s of the fully flooded test. With the exception of the ball counterface for NZO4 under marginally lubricated contact, all the balls under both conditions undergo abrasive wear, as indicated by scratches of various sizes in the sliding direction. For the ball counterface of NZO4 under marginally lubricated contact, wear occurred by mild polishing, thereby showing the lowest wear volume, as can be seen in Fig. 9.

4 Conclusion

Nitrogen-doped ZnO thin films were deposited on 304L stainless steel substrate using MOCVD through the pyrolysis of zinc acetate and ammonium acetate in different ratios at a temperature of 420 ℃. RBS indicated that the expected elements were present in the thin film, and the stoichiometric ratio of N:Zn:O was estimated to be 1:5:4 in all the films. The XRD

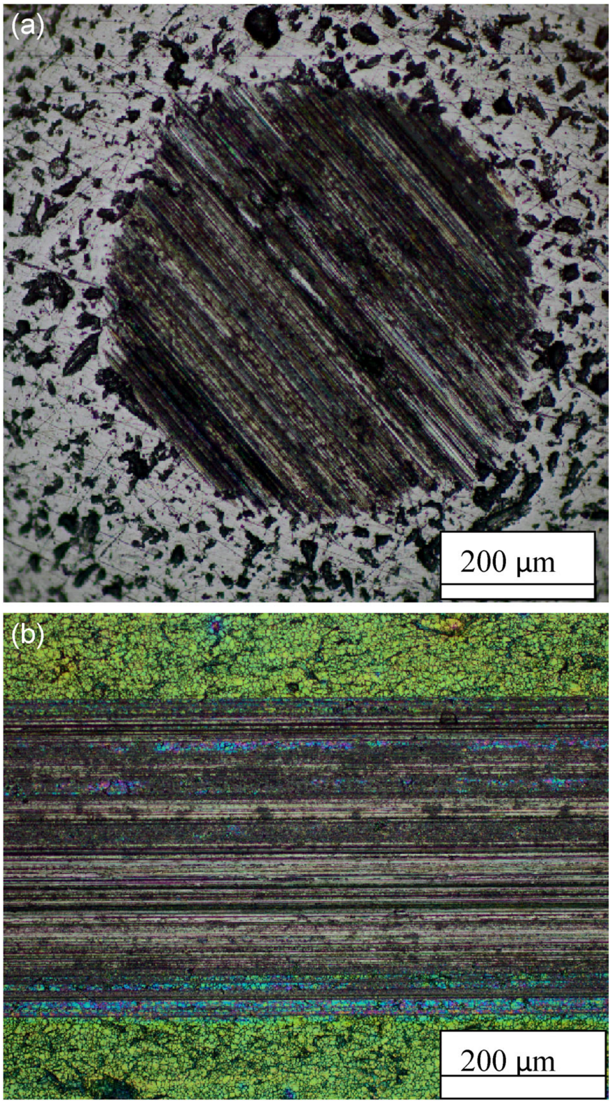

Fig. 13 Typical optical micrographs of (a) ball counterface and (b) nitrogen-doped ZnO thin film under fully flooded condition.

result demonstrated the nanocrystalline nature of the films with a hexagonal structure, which mirrored that of hexagonal wurtzite ZnO, in which *c* axis-oriented (002) plane perpendicular to the substrate dominated.

The friction and wear behaviors of 304L stainless steel and nitrogen-doped ZnO thin films were studied by using high-frequency reciprocating rig, sliding under marginally lubricated, and fully flooded conditions. The tests were conducted with unformulated synthetic PAO10 as lubricant. Nitrogen-doped ZnO thin films were able to provide friction reduction compared with the substrate under marginal lubrication, although the film was worn through in two samples (ZO and ZNO1) of the films. Under the fully flooded condition, three of the N-doped ZnO thin films (ZO, NZO2, and NZO4) were able to provide friction reduction only during the run-in period. After the run-in period, the coefficient of friction for the substrate became lower (after a good transfer layer had formed) than that of the nitrogen-doped ZnO thin films.

Most of the wear was produced in the Al alloy ball counterface as the wear on the flats was minimal coupled with material transfer from the ball counterface. The wear behavior of the ball counterface was strongly related to the friction behavior. Under the marginally lubricated condition, nitrogen-doped ZnO thin films showed a significant effect in protecting the ball counterface. Indeed, wear volume was reduced compared with that of the substrate. Under the fully flooded condition, with the exception of one of the films (NZO1), a reduction in the ball wear volume of the nitrogen-doped ZnO thin films was also observed compared with that of the substrate. In all the ball counterfaces for nitrogen-doped ZnO thin films under both marginally lubricated and fully flooded conditions, wear occurred through the abrasive mechanism of various degrees or mild polishing. Thus, superfluous lubrication of nitrogen-doped ZnO thin films is not necessary to reduce friction and wear.

Acknowledgements

This work was supported by U.S. Department of Energy, Energy Efficiency and Renewable Energy, Office of Vehicle Technologies, under contract DE-AC02-06CH11357. The authors are also grateful to Center for Research and Development, Obafemi Awolowo University, Ile-Ife, Nigeria, for RBS and XRD analyses.

References

[1] Khorramain B A, Iyer G R, Kodali S, Natarajan P, Tupil R. Review of antiwear additives for cranckcase oils. *Wear* **169**: 87–95 (1993)

[2] Zhou X D, Wu D M, Shi H Q, Fu X, Hu Z S, Wang X B, Yan F Y. Study on the tribological properties of surfactant-modified MoS_2 micrometer spheres as an additive in liquid paraffin. *Tribol Int* **40**: 863–868 (2007)

[3] Song X, Qiu Z, Yang X, Gong H, Zheng S, Cao B, Wang H, Möhwald H, Schukin D. Submicron-lubricant based on crystalline Fe_3O_4 spheres for enhanced tribology performance. *Chem Mater* **26**: 5113–5119 (2014)

[4] Harnandez-Battez A, Gonzàlez R, Viesca J L, Fernandez J E, Fernandez J M D, Machado A, Chou R, Riba J. CuO, ZrO_2 and ZnO nanoparticles as antiwear additive in oil lubricants. *Wear* **265**: 422–428 (2008)

[5] Radice S, Mischler S. Effect of electrochemical and mechanical parameters on the lubrication behavior of Al_2O_3 nanoparticles in aqueous suspension. *Wear* **261**: 1032–1041 (2006)

[6] Hu X, Gong H, Wang Y, Chen Q, Zhang J, Zheng S, Yang X, Cao B. Laser induced reshaping of particles aiming at energy saving applications. *J Mater Chem* **22**: 15947–15952 (2012)

[7] Zabinski J S, Corneille J, Prasad S V, Mc Devitt N T, Bultman J B. Lubricious zinc oxide films: Synthesis, characterization and tribological behavior. *J Mater Sci* **32**: 5313–5319 (1997)

[8] Prasad S V, Zabinski J S. Tribological behavior of nano-crystalline zinc oxide films. *Wear* **203–204**: 498–506 (1997)

[9] Prasad S V, Walck S D, Zabinski J S. Microstructural evolution in lubricious ZnO films grown by pulsed laser deposition. *Thin Solid Films* **360**: 107–117 (2000)

[10] Zabinski J S, Sanders J H, Nainaparampil J, Prasad S V. Lubrication using a microstructurally engineered oxide: Performance and mechanism. *Tribol Lett* **8**: 103–116 (2000)

[11] Chai C, Lu X, He D. Atomic layer deposition of zinc oxide films: Effects of nanocrystalline characteristics on tribological performance. *Surf Coat Technol* **207**: 361–366 (2012)

[12] Hu X, Gong H, Wang Y, Chen Q, Zhang J, Zheng S, Yang X, Cao B. Laser induced reshaping of particles aiming at energy saving applications. *J Mater Chem* **22**: 15947–15952 (2012)

[13] Li W, Zheng S, Wang P, Chen Q, Song X, Cao B. Preparation of ZnO nanoparticles with enhanced antifriction properties. *Asian J Chem* **24**: 2753–2756 (2012)

[14] Prasad S V, Nainaparampil J J, Zabinski J S. Tribological behavior of alumina doped zinc oxide films grown by pulsed laser deposition. *J Vac Sci Technol A* **20**: 1738–1743 (2002)

[15] Penkov O V, Lee D H, Kim H, Kim D E. Frictional behavior of atmospheric plasma jet deposited carbon-ZnO composite coatings. *Composite Sci Technol* **77**: 60–66 (2013)

[16] Wang S, Ge S, Zhang D. Comparison of tribological behavior of nylon composite filled with zinc oxide particles and whiskers. *Wear* **266**: 248–254 (2009)

[17] Liu B, Yang Z, Zhou J. Tribological behavior of polyimide zinc oxide hybrid films. *Adv Mater Res* **106**: 438–445 (2010)

[18] Chakraborty H, Sinha A, Mukherjee N, Ray D, Chattopadhyay P P. A study of nanocrystalline and tribological behavior of multifunctional ZnO/PMMA nanocomposite. *Mater Lett* **93**: 137–140 (2013)

[19] Chang B P, Akil H M, Nasir R B M. Composite study of micro- and nano-ZnO reinforced UHMWPE composites under dry sliding. *Wear* **297**: 1120–1127 (2013)

[20] Duan G, Hu X, Song X, Qiu Z, Gong H, Cao B. Morphology evolution of ZnO submicron particles induced by laser irradiation and their enhanced tribology properties by compositing with Al_2O_3 nanoparticles. *Adv Eng Mater* **17**: 341–348 (2015)

[21] Qin H, Li W, Xia Y, He T. Photocatalytic activity of heterostructures based on ZnO and N-doped ZnO. *ACS Appl Mater Interfaces* **3**: 3152–3156 (2011)

[22] Macias-Sanchez J J, Hinojosa-Reyes L, Caballero-Quintero A, de la Cruz W, Ruiz-Ruiz E, Hernandez-Ramireza A, Guzman-Mar J L. Synthesis of nitrogen-doped ZnO by sol gel method: Characterization and its application on visible photocatalytic degradation of 2, 4-D and picloram herbicides. *Photochem Photobiol Sci* **14**: 536–542 (2015)

[23] Herring N P, Panchakarla L S, El-Shall M S. P-type nitrogen-doped ZnO nanostructures with controlled shape and doping level by facile microwave synthesis. *Langmuir* **30**: 2230–2240 (2014)

[24] Naouar M, Ka I, Gaidi M, Alawadhi H, Bessais B, El Khakani M A. Growth structure and optoelectronic properties tuning of nitrogen-doped ZnO thin films synthesized by means of reactive pulse laser deposition. *Mater Res Bull* **57**: 47–51 (2014)

[25] Allenic A, Guo W, Chen Y B, Zhao G Y, Pan X Q, Che Y, Hu Z D, Liu B. Synthesis and properties of p-type nitrogen-doped ZnO thin films by pulsed laser ablation of a Zn-rich Zn_3N_2 target. *J Mater Res* **22**: 2339–2344 (2007)

[26] Lavand A B, Malghe Y S. Synthesis, characterization and visible light photocatalytic activity of nitrogen-doped zinc oxide nanospheres. *J Asian Ceramic Soc* **3**: 305–310 (2015)

[27] Mbamara U S, Olofinjana B, Ajayi O O, Lorenzo-Martin C, Obiajunwa E I, Ajayi E O B. Friction and wear behavior of nitrogen-doped ZnO thin films deposited *via* MOCVD under dry contact. *Eng Sci Technol* **19**: 956–963 (2016)

[28] Ajayi O B, Akanni M S, Lambi J N, Jeynes C, Watt J F. Compositional studies of various metal oxide coatings on glass. *Thin Solid Films* **185**: 123–136 (1990)

[29] Ajayi O B, Ojo I A, Jeynes C. Preparation and characterization of MOCVD thin films of cadmium sulphide. *Thin Solid Films* **248**: 57–62 (1994)

[30] Adedeji A V, Eleruja M A, Ojo I A O, Djebah A, Osasona O, Olowolafe J O, Aladekomo J B, Ajayi E O B. Preparation and characterization of MOCVD ZnCdInS thin films. *Opt Mater* **14**: 345–349 (2000)

[31] Adedeji A V, Egharevba G O, Jeynes C, Ajayi E O B. Preparation and characterization of pyrolytically deposited (CO-V-O and Cr-V-O) thin films. *Thin Solid Films* **402**: 49–54 (2002)

[32] Ilori O O, Osasona O, Eleruja M A, Egharevba G O, Adegboyega G A, Chiodeli G, Boudreault G, Jeynes C, Ajayi E O B. Preparation and characterization of metallorganic chemical vapor deposited $Li_xMo_yO_z$ using a single source solid precursor. *Ionics* **11**: 387–391 (2005)

[33] Olofinjana B, Egharevba G O, Eleruja M A, Jeynes C, Adedeji A V, Akinwunmi O O, Taleatu B A, Mordi C U, Ajayi E O B. Synthesis and some properties of metal organic chemical vapor deposited molybdenum oxysulphide thin films. *J Mater Sci Technol* **26**: 552–557 (2010)

[34] Olofinjana B, Egharevba G, Teleatu B, Akinwunmi O, Ajayi E O. MOCVD of molybdenum sulphide thin film *via* single solid source precursor Bis-(Morpholinodithioato-S,S')-Mo. *J Mod Phys* **2** 341–349 (2011)

[35] Mbamara U S, Olofinjana B, Lorenzo-Martin C, Ajayi O O, Obiajunwa E I, Ajayi E O B. Surface statistical topographical properties of ZnO:N thin films deposited by MOCVD. *J NanoSci NanoEng* **1**: 18–22 (2015)

[36] Mbamara U S, Akinwunmi O O, Obiajunwa E I, Ojo I A O, Ajayi E O B. Deposition and characterization nitrogen-doped zinc oxide thin films by MOCVD using zinc acetate-ammonium acetate precursor. *J Mod Phys* **3**: 652–659 (2012)

[37] Xu W, Ye Z, Zhou T, Zhao B, Zhu L, Huang J. Low pressure MOCVD growth of p-type ZnO thin films by using NO as the dopant source. *J Cryst Growth* **265**: 133–136 (2004)

[38] Tan S T, Chen B J, Sun X W, Yu M B, Zhang X H, Chua S J. Realization of intrinsic p-type ZnO thin films by metal organic vapor deposition. *J Electron Mater* **34**: 1172–1176 (2005)

[39] Qu J, Blau P J, Zhang L, Xu H. Effect of multiple treatment of low-temperature colossal supersaturation on tribological characteristic of austenitic stainless steel. *Wear* **265**: 1909–1913 (2008)

[40] Schön J. Coefficient of friction for aluminum in contact with a carbon fiber epoxy composite. *Tribol* **137**: 395–404 (2004)

[41] Schön J. Coefficient of friction of composite delamination surfaces. *Wear* **237**: 77–89 (2000)

[42] Qu J, Blau P J, Jolly B C. Tribological properties of stainless steel treated by colossal carbon supersaturation. *Wear* **263**: 719–726 (2007)

[43] Lorenzo-Martin C, Ajayi O, Erdemir A, Fenske G R, Wei R. Effect of microstructure and thickness on the friction and wear behavior of CrN coatings. *Wear* **302**: 963–971 (2013)

[44] Budinski K G, Budinski M K. *Engineering Materials, Properties and Selection*. New Jersey (USA): Prentice Hall, 2002.

Bolutife OLOFINJANA. He received his bachelor, M.Sc., and Ph.D. degrees in enigineering physics from Obafemi Awolowo University, Ile-Ife, Nigeria in 1999, 2005, and 2011, respectively. He joined Obafemi Awolowo University as an assistant lecturer in the department of Physics and Engineering Physics. He is currently a senior lecturer in the same department. His research interests include surface modification for active control of friction and wear, and preparation and characterization of nano-structured materials for various applications.